IET Circuits, Devices & Systems

Research Article

IET Journals
The Institution of Engineering and Technology

Uncalibrated operational amplifier-based sensor interface for capacitive/resistive sensor applications

ISSN 1751-858X
Received on 1st April 2014
Accepted on 13th October 2014
doi: 10.1049/iet-cds.2014.0248
www.ietdl.org

Andrea De Marcellis ✉, *Giuseppe Ferri*, *Paolo Mantenuto*

Department of Industrial and Information Engineering and Economics, University of L'Aquila, 67100 L'Aquila, Italy
✉ *E-mail: andrea.demarcellis@univaq.it*

Abstract: In this paper, a new configuration of operational amplifier -based square-wave oscillator is proposed. The circuit performs an impedance-to-period (Z–T) conversion that, instead of a voltage integration typically performed by other solutions presented in the literature, is based on a voltage differentiation. This solution is suitable as first analogue uncalibrated front-end for capacitive and resistive (e.g. relative humidity and gas) sensors, working also, in the case of capacitive devices, for wide variation ranges (up to six capacitive variation decades). Moreover, through the setting of passive components, its sensitivity can be easily regulated. Experimental measurements, conducted on a prototype printed circuit board, with sample passive components and using the commercial capacitive humidity sensor Honeywell HCH-1000, have shown good linearity and accuracy in the estimation of capacitances, having a baseline or reaching a value ranging in a wide interval [picofarads–microfarads], as well as, with a lower accuracy, in the evaluation of more reduced variations of resistances, ranging from kiloohms to megaohms, also when compared with other solutions presented in the literature.

1 Introduction

Oscillators are well-known electronic circuits that generate a periodic AC waveform (e.g. sinusoidal or square-wave) whose output period is related to the employed passive component values. Typical design techniques are referred to the voltage-mode approach using operational amplifiers (OAs) and current-mode approach by employing second generation current conveyors. Oscillating circuits are largely employed in many research and application fields, such as telecommunications, measurement systems and, also, as first analogue interfaces for sensor applications [1–23]. Typically, oscillators are based on an $R-C$ integrating cell, providing a switching current source that charges and discharges a capacitor (e.g. a capacitive sensor), followed by a voltage hysteresis comparator. In sensor interface, when the resistive or capacitive sensing device shows a wide variation baseline or range, oscillators result to be the best solution [1, 2, 24–34]. In fact, their output period is directly linked to the measurand value; moreover, thanks to their impedance-to-period (Z–T) conversion, their utilisation as first analogue front-ends overcomes typical problems related to those interface circuits performing an impedance-to-voltage conversion (e.g. bridge-based topologies) more suitable for reduced variations of the measurand, especially in low-voltage low-power solutions [1, 2, 35–55].

In this paper, we propose a novel and low-cost circuit solution as uncalibrated 'OA'-based fully analogue interface, operating a Z–T conversion, that is, suitable mainly for wide range capacitive, but also for resistive floating sensors. The novelty of this solution, which employs a reduced number of active and passive components, concerns the use of a voltage differentiating cell instead of a voltage integrator, typical of the oscillators proposed in the literature. In this manner, the circuit shows also a better immunity from low-frequency disturbs (e.g. DC offsets and $1/f$ noise). Furthermore, it is possible to easily select the working range and set its sensitivity to sensor parameters through a suitable choice of passive components. Experimental measurements have been performed implementing the proposed solution through a prototype printed circuit board ('PCB') employing a low-cost high performances commercial 'OA' (i.e. OPA350 by Texas Instruments) together with high-accuracy sample capacitors and resistors emulating sensor behaviours. As a practical sensor application example, the interface circuit has been employed for the detection of the percentage relative humidity ('RH%') through the use of a commercial capacitive sensor (i.e. HCH-1000 Series by Honeywell). Achieved measurement results have shown good linearity and accuracy, as well as a reduced estimation error, especially with respect to capacitive evaluations, also because of the circuit simplicity, validating the correct functionality of the proposed interface.

2 Proposed interface: circuit theory and behavioural analysis

The schematic circuit of the proposed oscillator is shown in Fig. 1. The implemented interface is very simple, consisting of six resistors, a capacitor and only two active components: the first, 'OA_1', is connected in an inverting voltage differentiator configuration, whereas the second, 'OA_2', works as an inverting hysteresis voltage comparator which provides the output square waveform. Through a suitable closed loop, which avoids any system calibration, resistive or capacitive sensors are excited by the generated AC signal. In addition, it is possible to easily set the interface working range through external parameters (only resistances) which allow also to fix the sensitivity of the readout circuit.

Fig. 2 shows the voltage time behaviour at the main circuit nodes, from which the differentiating effect on V_C can be seen. The oscillating condition is guaranteed by a proper choice of the voltage divider values (R_1, R_2), which creates the suitable threshold levels used by the comparator 'OA_2' to switch between its two saturation voltage limits. In particular, it is important to consider also that, in order to perform the correct comparison between V_A and V_C voltage signals at 'OA_2' input nodes (since V_C tends to V_B), the employed passive components have to be suitably chosen so to verify the following relationship

$$|V_B| > |V_A| \tag{1}$$

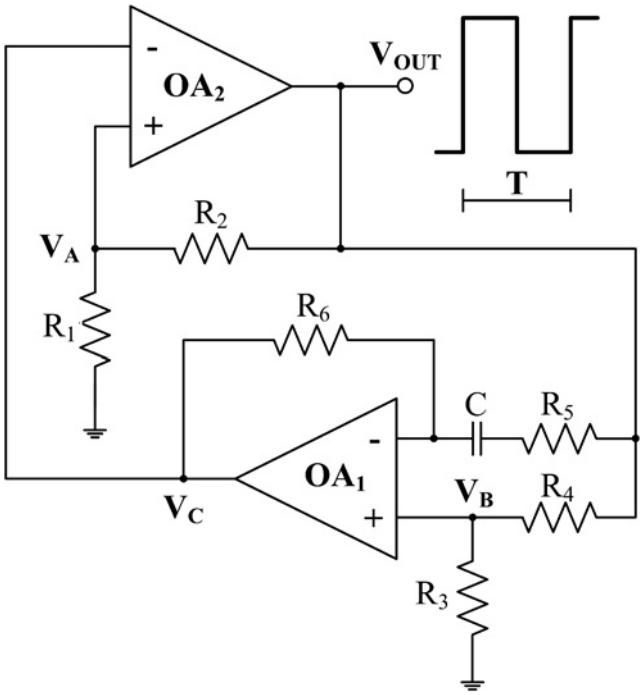

Fig. 1 *Block scheme of the proposed capacitive (C)/resistive (R_5 or R_6) sensor interface*

Through a straightforward circuit analysis, considering ideal 'OAs', it is possible to achieve the following expression for the period T, revealed at V_{OUT} node

$$T = 2CR_5 \ln\left(\frac{(R_5/R_6)A - 2B}{(R_5/R_6)A}\right) \tag{2}$$

being A and B defined, respectively, as

$$A = \left(\frac{R_3}{R_3 + R_4} - \frac{R_1}{R_1 + R_2}\right) \tag{3}$$

$$B = \frac{R_4}{R_3 + R_4} \tag{4}$$

From (2) it is evident the direct proportionality between the output period and capacitance C, so the interface is particularly suitable for capacitive sensor applications, but can also be employed, under particular conditions about the resistance values, considering R_5 or R_6 as a resistive sensor. Moreover, from (2) it can be highlighted

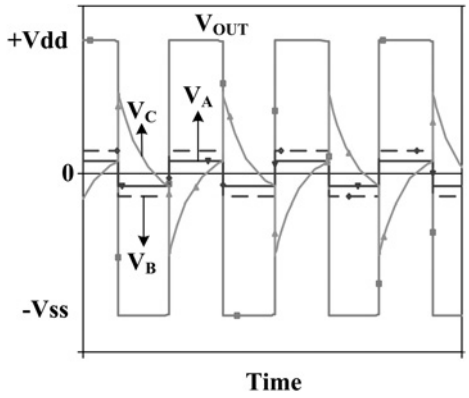

Fig. 2 *Typical time responses evaluated at main interface nodes*

the fact the output period T is completely independent from the chosen supply voltage so providing to the circuit a better immunity to power supply drifts and variations.

To achieve a better circuit characterisation, interface sensitivities, determined with respect to the possible passive parameter (i.e. C, R_5 and R_6) variations, have been evaluated. Reminding that sensitivity is calculated as the output signal variation (here referred as the output square waveform period T) with respect to the measurand change [56], starting from (2), the following relationships have been derived

$$S_C = \frac{\partial T}{\partial C} = 2R_5 \ln\left(\frac{(R_5/R_6)A - 2B}{(R_5/R_6)A}\right) \tag{5}$$

$$S_{R_5} = \frac{\partial T}{\partial R_5} = 2C\left[\ln\left(\frac{(R_5/R_6)A - 2B}{(R_5/R_6)A}\right) + \frac{2B}{(R_5/R_6)A - 2B}\right] \tag{6}$$

$$S_{R_6} = \frac{\partial T}{\partial R_6} = 4BC\left(\frac{R_5/R_6}{A(R_5/R_6) - 2B}\right) \tag{7}$$

As expected, with respect to capacitance measurand variations (see (5)), sensitivity assumes a constant value which depends only on the employed passive component values. This, obviously, means that it can be maximised by properly sizing the other circuit passive parameters, always according to the oscillation condition expressed in (1). On the contrary, regarding resistive variations, as seen in (6) and (7), sensitivity value strictly depends on both the employed passive components and the same sensor value (i.e. it is not a constant value, but is related to the circuit operating point). In this case, in fact, the sensitivity is nearly inversely proportional to the resistive sensor value.

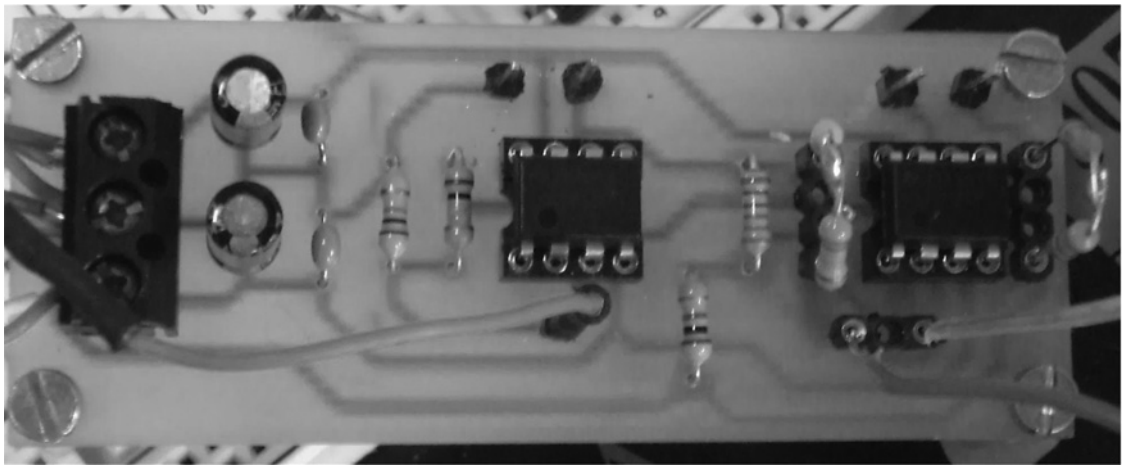

Fig. 3 *Photograph of the fabricated prototype PCB with commercial discrete components*

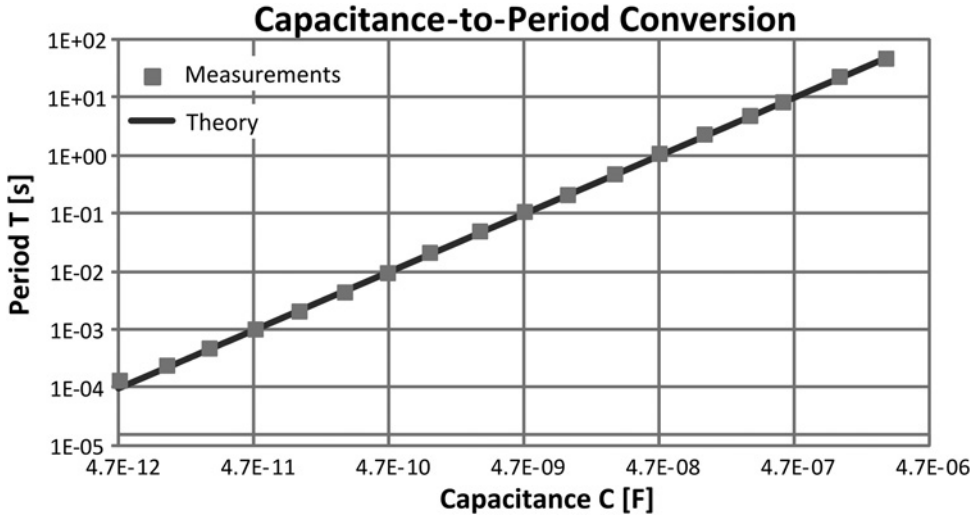

Fig. 4 *Theoretical responses and measurement results related to the period T of the output square waveform against sample capacitance C*

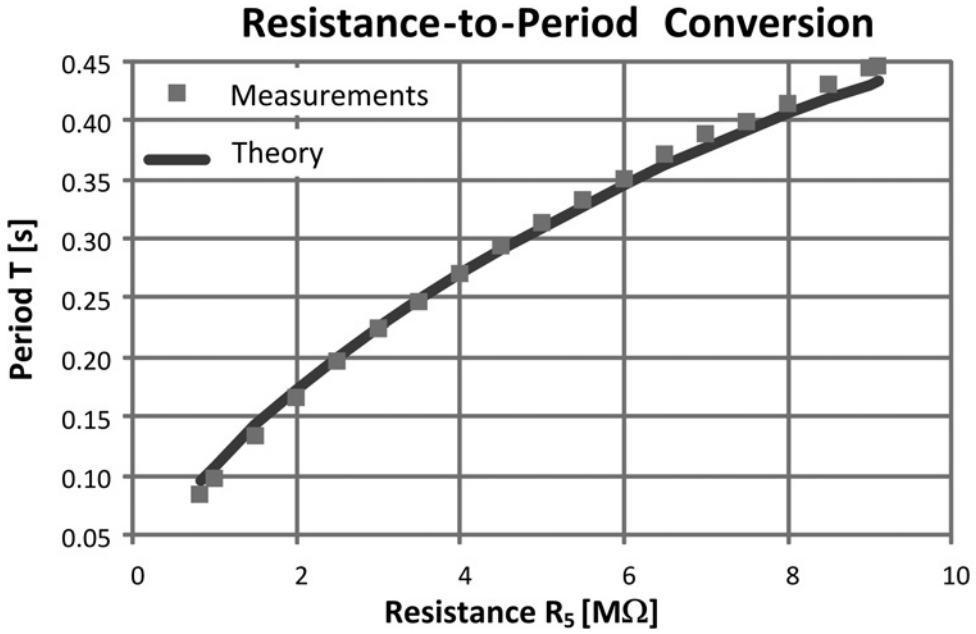

Fig. 5 *Theoretical responses and measurement results related to the period T of the output square waveform against sample resistance R_5*

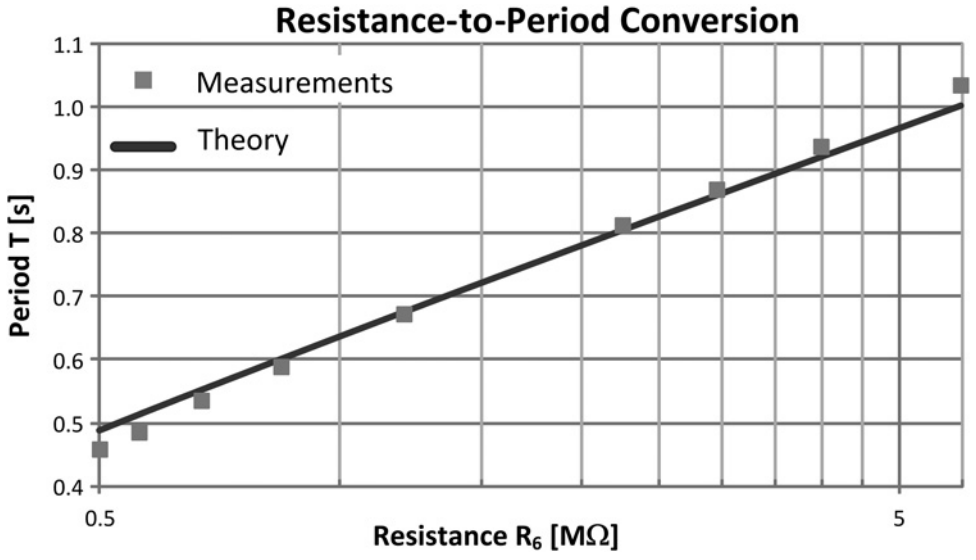

Fig. 6 *Theoretical responses and measurement results related to the period T of the output square waveform against sample resistance R_6*

3 Prototyping and experimental characterisation

Experimental measurements have been conducted on the fabricated 'PCB', whose photograph is reported in Fig. 3, with high-accuracy sample resistors and capacitors (emulating sensors). To achieve better features by the proposed circuit, OPA350 active component has been employed as a high performance 'OA', especially in terms of low-offset, low-noise, high slew-rate

Table 1 Main performances comparison of the proposed interface circuit with other solutions presented in the literature for resistive and/or capacitive sensors

Reference	C_{SENS} kind and dynamic range, F	R_{SENS} kind and dynamic range, Ω	Number and kind of active components	Number and kind of passive components	Sensitivity	Accuracy (relative error %)
this work	C floating: 4.7 p–2.2 μ	R_5 floating: 820 k–9.1 M R_6 floating: 500 k–5.95 M	two OA	six R one C	C floating: 21 μs/pF R_5 floating: 50–90 ms/MΩ R_6 floating: 170–900 ms/MΩ	C floating: <± 3% R_5 floating: <± 4% R_6 floating: <± 4%
[5]	C floating: 1–47 p	R floating: 100 k–100 G	four OA; one EX-OR	three R 2 C	N/A	R floating: <± 5% C floating: <± 15%
[11]	C grounded: 13 a–10.7 n	R floating: 5–11.5 M	one inverter; three buffer; two comparators; and one XOR	one crystal oscillator one R one C	C grounded: 7 μs/pF R floating: 500 μs/MΩ	N/A
[13]	C floating: 0–33 p	R floating: 470 k–100 G	four operational transconductance amplifier (OTA) and one EX-OR	three R two C	R floating: 320 μs/MΩ C floating: N/A	R floating: <± 3.9% C floating: <± 1%
[14]	–	R grounded: 1 k–10 M	one logarithmic converter; three anti-aliasing filter; three offset compensator; three analogue-to-digital converter (ADC); one digital-to-analogue converter (DAC); two band-pass filter; one square-root circuit; one digital proportional integral derivative controller (PID) controller; and one digital interface	N/A	N/A	N/A
[18]	C floating: 10 p–1 μ	R floating: 10 M–1 G R grounded: 150 k–1.5 M	two OTA	eight R one C	C floating: 3.5 μs/pF R floating: 1 ÷ 130 μs/MΩ R grounded: 350 ÷ 950 μs/MΩ	C floating: <± 6% R floating: <± 3% R grounded: <± 3%
[20]	–	bridge of R: R_0 = 10 k	one multiplexer; one analogue front-end; one low-pass filter; one ΣΔ-ADC; one ADC; one voltage reference; one 24 bit counter; one flag register; and one inter integrated circuit (I2C) interface	N/A	625 V_{out}/V_{in}	8 bit
[21]	C floating: 1–300 p	R floating: 250–50 k	N/A	N/A	R floating: 50 μs/VC floating: 10 μs/pF	N/A
[22]	–	R grounded: 0.7–7 k	two OA	four R one C	R grounded: 330 μs/kΩ	N/A
[23]	C floating: 0.8–1.2 p	–	four OTA; one OA; five switch; and one AND	three C	C floating: 15–47 μs/pF	C floating: <±0.6%
[31]	C floating: 1–22 p	R floating: 10 k–1 G	four OTA and one AND	seven R three C	R floating: 330 μs/kΩ C floating: N/A	R floating: <±10% C floating: <±10%
[32]	C floating: 16–40 p	–	one multiplexer; one charge pump; one voltage controlled oscillator (VCO); one DAC; one voltage reference; one integrator; one voltage gain amplifier (VGA); one sample and hold (S&H); one clock generator; one sensor bus interface; and one erasable programmable read only memory	N/A	C floating: 20.8 μV/fF 1.25 mV/fF	N/A
[33]	C floating: 1–300 p	–	two OA; one logic control; and five switch	four C	N/A	C floating: <±0.5%
[34]	–	R grounded: 150–85 M	two OA; one multiplexer; two current multiplier; one current divider; one control logic; two AND; one counter; one global reset; one reset logic; one decoder; one register; and six switch	one R two C	N/A	N/A
[38]	–	bridge of R: R_0 = 3 k	two OA; 30 switch; one switch control; one phase selection; and two divider	eight R seven C	N/A	<±0.1%
[45]	–	R_4 floating: 0.1–1 k R_3 grounded: 1–11 k	three OA	R floating: six R and two C R grounded: five R and one C	R floating: 0.8 ms/kΩ R grounded: 40 ms/kΩ	N/A
[46]	C floating: N/A	R grounded: N/A	two OA	three R and one C	N/A	N/A
[49]	C floating: 1.5–2.5 p	–	eight switches; one OA; two comparators; four flip-flops; and 13 digital logic gates	four C	N/A	<±0.13%
[50]	–	R floating: 99.6–999	one external clock generator; three external current generators; three switches; four OA; two comparators; and two digital logic gates	five R; three C; and two diodes	R floating: 81 μs/kΩ	<±0.9%
[53]	C floating: 0.5–3 p	–	one OA; one transmission gate; one comparator; one delay block; one one-shot circuit block; and one digital logic gate	one C	C floating: 4 μs/pF	<±8.3%

('SR'), high gain bandwidth product (GBW) and, above all, powered at a single supply voltage equal to +5 V. More in detail, this active component shows the following main characteristics: complete input/output dynamic range, wide 'GBW' (38 MHz), high 'SR' (22 V/μs), low input noise (5 nV/(Hz)$^{1/2}$) and very low total harmonic distortion (0.0006%).

Measurement results have confirmed the system capability to work in a large interval of sensor variations (e.g. kiloohms (kΩ) ÷ megaohms (MΩ) or picofarads (pF) ÷ microfarads (μF), settable ranges) and have shown a good agreement with the theoretical expectations (ideal behaviour) determined by (2), especially related to the case of capacitive sensors.

More in detail, by setting $R_1 = 10$ kΩ, $R_2 = 100$ kΩ, $R_3 = 1$ kΩ, $R_4 = 9$ kΩ, $R_5 = 2.2$ MΩ and $R_6 = 1.35$ MΩ, the proposed interface estimates, with a good linearity and accuracy, wide-range capacitance values (about six decades, from 4.7 pF to 2.2 μF, covering different kinds of capacitive sensors), as shown in Fig. 4. The interface can be also employed to reveal and quantify, even if with a worst accuracy, about one-decade resistive variation, in particular from 820 kΩ to 9.1 MΩ, considering R_5 as resistive sensor as reported in Fig. 5, by setting $R_1 = 10$ kΩ, $R_2 = 100$ kΩ, $R_3 = 1$ kΩ, $R_4 = 9$ kΩ, $R_6 = 499$ kΩ, $C = 10$ nF and from 500 kΩ to 5.95 MΩ, considering R_6 as resistive sensor as depicted in Fig. 6, by setting $R_1 = 10$ kΩ, $R_2 = 100$ kΩ, $R_3 = 1$ kΩ, $R_4 = 9$ kΩ, $R_5 = 10$ MΩ and $C = 10$ nF. In this sense, the capacitance value is directly proportional to the output waveform period T, whereas, unfortunately, the resistance value affects also the oscillation condition expressed by (1) and the logarithm argument of (2).

According to the theoretical calculations expressed by (5)–(7), in the here presented configurations, sensitivity values have been set to about 21 μs/pF considering C as capacitive sensors and 50–90 ms/MΩ and 170–900 ms/MΩ taking into account R_5 and R_6 as resistive sensors, respectively.

In addition, in Table 1, the main performances of the proposed circuit topology are summarised and compared with other similar solutions presented in the literature. As it can be seen, our oscillator shows good characteristics, in particular: wide dynamic range for capacitive sensors, reduced number of active and passive components, simple circuitry complexity and easiness of integration as an application specific integrated circuit (ASIC) in a standard 'CMOS' technology, high sensitivity (settable) and good accuracy, capability to work also with low supply voltage since its output frequency is independent from the employed power supply (i.e. a better immunity to the battery discharge in portable applications).

Furthermore, in comparison with the single 'OA'-based a stable multivibrator, it is possible to easily set the circuit working range and its sensitivity to sensor parameters through a suitable choice of passive components. This allows to have more degrees of freedom as a function of the employed sensor and its main characteristics, especially in terms of dynamic range, sensitivity and resolution. On the contrary, the main disadvantage of the proposed circuit is related to the fact that linear responses between the output period and the sensor parameter (C, R_5, R_6) are ensured only when capacitive sensors are employed (see (2)). On the other hand, another more general drawback related to the introduced voltage differentiation approach is in the possibility to provide sometimes few unwanted spikes in the time responses.

4 Experimental measurements with a commercial capacitive humidity sensor

Experimental tests have been conducted through the use of the commercial capacitive RH% sensor HCH-1000 Series by Honeywell, utilised to reveal and quantify the 'RH%' time variations in a test closed chamber, where a mixture of dry and wet air has been fluxed. Sensor datasheet underlines that sensor behaviour is characterised by a reduced hysteresis cycle, so a number of experiments have been conducted so to better characterise both the sensor and the readout circuit. The 'RH%' reference values have been achieved by the HTD-625 High Accuracy Thermo-Hygrometer, having a resolution of 0.1%RH and an accuracy of ±2%RH.

Moreover in this case, different tests have been conducted utilising, as 'OA', the high performances OPA350 by Texas Instruments, supplied at +5 V (i.e. a single supply voltage) and considering the same circuit settings reported above as concerning the capacitance-to-period conversion measurements (see Section 3 and referred to Fig. 4). In this manner, a maximum voltage lower than 2 V has been achieved to excite the sensor, according to its datasheet. By imposing this operative conditions, new tests and measurements have been conducted. More in detail, in order to deeply analyse sensor hysteresis, a mixture profile of increasing (up to 80%) and decreasing steps related to 'RH%' variations, with respect to the dry air reference, has been employed. The achieved measurement results are in good agreement with each other, also for a sudden change between dry air ('RH%' = 0) and a fixed humidity reference. On the other hand, experimental data, reported in Fig. 7, show that both the sensor and the interface responses, for the same 'RH%' level, assume about the same values so that the sensing device hysteresis effect can be considered negligible and also the estimated capacitance level is closer to the expected one, also according to that one reported in the sensor datasheet.

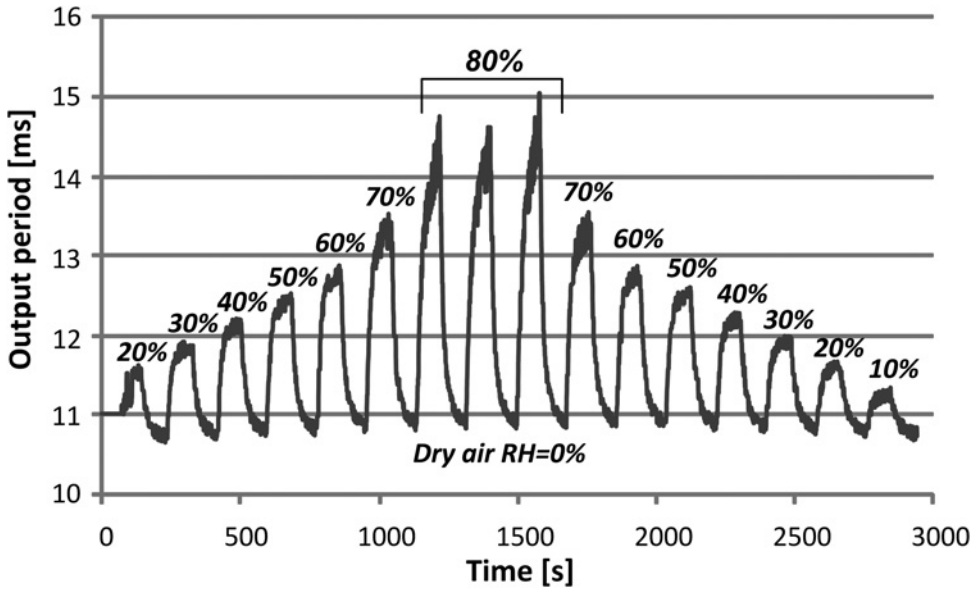

Fig. 7 *Experimental measurement showing the output period T against RH %; the circuit employs a commercial capacitive humidity sensor and OPA350 as OA single supplied at +5 V (i.e. C–T conversion)*

5 Conclusions

In this paper, a simple uncalibrated 'OA'-based oscillating circuit, suitable as first analogue interface for capacitive/resistive floating sensor applications, has been presented. The proposed solution is based on a differentiating cell instead of the classical integrating one. The square-wave output signal, which offers a better immunity from low-frequency noise (i.e. $1/f$ and DC offsets), provides an easy way to process the sensor impedance allowing a simple data acquisition and a direct elaboration through low-cost digital processing systems. It is constituted by a simple topology, implemented by only two 'OAs', resulting suitable for the integration on chip, in a standard 'CMOS' technology, through a proper low-voltage low-power circuit design. Its validity has been demonstrated through several experimental measurements using the fabricated discrete components prototype 'PCB', sample capacitors and resistors emulating sensors, commercial high performances 'OAs' and a capacitive humidity sensor as an application example. Considering the good linearity, the possibility to easily regulate the system sensitivity, the wide output range (also up to six capacitance variation decades) and considering also a suitable comparison with other similar interfaces presented in the literature, we believe that the proposed interface circuit can be considered as a suitable solution for portable sensor interfacing applications.

6 Acknowledgments

The authors thank Gianni Cirella for his help in the 'PCB' fabrication and Stefano Antonini for his contribution in the experimental tests.

7 References

1 De Marcellis, A., Ferri, G.: 'Analog circuits and systems for voltage-mode and current-mode sensor interfacing applications' (Springer, 2011, Dordrecht, 1st edn.)
2 De Marcellis, A., Ferri, G., Mantenuto, P.: 'Resistive sensor interfacing', in Reig, C., Cardoso, S., Mukhopadhyay, S.C. (Eds.): 'Giant magnetoresistance (GMR) sensors' (Springer, 2013, Heidelberg, 1st edn.), pp. 71–102
3 Daliri, M., Maymandi-Nejad, M.: 'Analytical model for CMOS cross-coupled LC-tank oscillator', *IET Circuits Devices Syst.*, 2014, **8**, pp. 1–9
4 Moradzadeh, H., Azhari, S.J.: 'Low-voltage low-power rail-to-rail low-Rx wideband second generation current conveyor and a single resistance-controlled oscillator based on it', *IET Circuits Devices Syst.*, 2011, **5**, pp. 66–72
5 De Marcellis, A., Depari, A., Ferri, G., *et al.*: 'A CMOS integrable oscillator-based front end for high-dynamic-range resistive sensors', *IEEE Trans. Instrum. Meas.*, 2008, **57**, pp. 1596–1604
6 Depari, A., Flammini, A., Marioli, D., *et al.*: 'Uncalibrated integrable wide-range single-supply portable interface for resistance and parasitic capacitance estimation', *Sens. Actuators B*, 2008, **132**, pp. 477–484
7 Vlassis, S., Laopoulos, T., Siskos, S.: 'Pressure sensors interfacing circuit with digital output', *IET Circuits Devices Syst.*, 1998, **145**, pp. 332–336
8 Ferri, G., De Marcellis, A., Di Carlo, C., *et al.*: 'A second generation current conveyor (CCII)-based low-voltage low-power read-out circuit for DC-excited resistive gas sensors', *IEEE Sens. J.*, 2009, **9**, pp. 2035–2041
9 Depari, A., De Marcellis, A., Ferri, G., Flammini, A.: 'A complementary metal oxide semiconductor-integrable conditioning circuit for resistive chemical sensor management', *IOP Meas. Sci. Technol.*, 2011, **22**, pp. 2–7
10 Azarmehr, M., Rashidzadeh, R., Ahmadi, M.: 'Low-power oscillator for passive radio frequency identification transponders', *IET Circuits Devices Syst.*, 2012, **6**, pp. 79–84
11 Lu, J.H.L., Inerowicz, M., Sanghoon, J., Jong-Kee, K., Byunghoo, J.: 'A low-power wide-dynamic-range semi-digital universal sensor readout circuit using pulsewidth modulation', *IEEE Sens. J.*, 2011, **11**, pp. 1134–1144
12 Pathak, J.K., Singh, A.K., Senani, R.: 'Systematic realisation of quadrature oscillators using current differencing buffered amplifiers', *IET Circuits Devices Syst.*, 2011, **5**, pp. 203–211
13 Ferri, G., De Marcellis, A., Di Carlo, C., *et al.*: 'A single-chip integrated interfacing circuit for wide-range resistive gas sensor arrays', *Sens. Actuators B*, 2009, **143**, pp. 218–225
14 Barrettino, D., Graf, M., Taschini, S., Hafizovic, S., Hagleitner, C., Hierlemann, A.: 'CMOS monolithic metal-oxide gas sensor microsystems', *IEEE Sens. J.*, 2006, **6**, pp. 276–286
15 Rastrello, F., Placidi, P., Scorzoni, A.: 'A system for the dynamic control and thermal characterization of ultra low power gas sensors', *IEEE Trans. Instrum. Meas.*, 2011, **60**, pp. 1876–1883
16 Depari, A., Flammini, A., Marioli, D., *et al.*: 'A new and fast-readout interface for resistive chemical sensors', *IEEE Trans. Instrum. Meas.*, 2010, **59**, pp. 1276–1283
17 De Marcellis, A., Ferri, G., Mantenuto, P.: 'A novel uncalibrated read-out circuit for floating capacitive and grounded/floating resistive sensor measurement'. Proc. Eurosensors XXVI, Cracow, Poland, September 2012, pp. 253–256
18 De Marcellis, A., Ferri, G., Mantenuto, P., Depari, A., Flammini, A., Sisinni, E.: 'A new 0.35 μm CMOS electronic interface for wide range floating capacitive and grounded/floating resistive sensor applications', *Microelectron. J.*, 2014, **45**, pp. 910–920
19 De Marcellis, A., Ferri, G., Mantenuto, P.: 'A novel OA-based oscillating circuit for uncalibrated capacitive and resistive sensor interfacing applications'. Proc. IMCS, Nuremberg, Germany, May 2012, pp. 1707–1709
20 Zimmermann, M., Volden, T., Kirstein, K.U., *et al.*: 'A CMOS-based integrated-system architecture for a static cantilever array', *Sens. Actuators B*, 2008, **134**, pp. 254–264
21 Universal Transducer Interface UTI Datasheet, Smartec, 2008. Available at on-line resource http://www.smartec.nl
22 De Marcellis, A., Cubells-Beltrán, M.D., Reig, C., *et al.*: 'Quasi-digital front-ends for current measurement in integrated circuits with giant magnetoresistance technology', *IET Circuits Devices Syst.*, 2014, **8**, pp. 291–300
23 Bruschi, P., Nizza, N., Piotto, M.: 'A current-mode, dual slope, integrated capacitance-to-pulse duration converter', *IEEE J. Solid-State Circuits*, 2007, **42**, pp. 1884–1891
24 Ferri, G., Stornelli, V., De Marcellis, A., Flammini, A., Depari, A.: 'Novel CMOS fully integrable interface for wide-range resistive sensor arrays with parasitic capacitance estimation', *Sens. Actuators B*, 2008, **130**, pp. 207–215
25 Bhattacharyya, P., Basu, P.K., Saha, H., Basu, S.: 'Fast response methane sensor based on Pd(Ag)/ZnO/Zn MIM structure', *IEEE Sens. Lett.*, 2006, **4**, pp. 371–376
26 Daungdaw, S., Prangsri-Aroon, S., Viravathana, P., Wongchaisuwat, A., Eamchotchawalit, C.: '$LaCoO_3$ perovskites for CO sensing', *Sens. Lett.*, 2013, **11**, pp. 556–559
27 Kosterev, A.A., Bakhirkin, Y.A., Tittel, F.K., McWhorter, S., Ashcraft, B.: 'QEPAS methane sensor performance for humidified gases', *Appl. Phys. B*, 2008, **92**, pp. 103–109
28 Balachandran, M.D., Shrestha, S., Agarwal, M., Lvov, Y., Varahramyan, K.: 'SnO2 capacitive sensor integrated with microstrip patch antenna for passive wireless detection of ethylene gas', *Electron. Lett.*, 2008, **44**, pp. 464–466
29 Sahraoui, Y., Barhoumi, H., Maaref, A., Jaffrezic-Renault, N.: 'A novel capacitive biosensor for urea assay based on modified magnetic nanobeads', *Sens. Lett.*, 2011, **9**, pp. 2141–2146
30 Radosavljevic, G., Pochia, M.M., Rosca, D., Blaž, N., Maric, A.: 'Capacitive low temperature Co-fired ceramic fluidic sensor', *Sens. Lett.*, 2013, **11**, pp. 646–649
31 De Marcellis, A., Depari, A., Ferri, G., Flammini, A., Sisinni, E.: 'A CMOS integrated low-voltage low-power time-controlled interface for chemical resistive sensors', *Sens. Actuators B*, 2013, **179**, pp. 313–318
32 Mason, A., Chavan, A.V., Wise, K.D.: 'A mixed-voltage sensor readout circuit with on-chip calibration and built-in self-test', *IEEE Sens. J.*, 2007, **7**, pp. 1225–1232
33 Heidary, A., Meijer, G.C.M.: 'Features and design constraints for an optimized SC front-end circuit for capacitive sensors with a wide dynamic range', *IEEE J. Solid-State Circuits*, 2008, **43**, pp. 1609–1616
34 Jayaraman, B., Bath, N.: 'High precision 16 bit readout gas sensor interface in 0.13 μm CMOS'. Proc. IEEE ISCAS, New Orleans, USA, May 2007, pp. 3071–3074
35 Mantenuto, P., De Marcellis, A., Ferri, G.: 'Uncalibrated analog bridge-based interface for wide-range resistive sensor estimation', *IEEE Sens. J.*, 2012, **12**, pp. 1413–1414
36 Liu, B., Cai, L., Zhu, J., Kang, Q., Zhang, M., Chen, X.: 'On-chip readout circuit for nanomagnetic logic', *IET Circuits Devices Syst.*, 2014, **8**, pp. 65–72
37 Johnson, C.D., Chen, C.: 'Bridge-to-computer data acquisition system with feedback nulling', *IEEE Trans. Instrum. Meas.*, 1990, **39**, pp. 531–534
38 Van der Goes, F.M.L., Meijer, G.C.M.: 'A simple accurate bridge-transducer interface with continuous autocalibration', *IEEE Trans. Instrum. Meas.*, 1997, **46**, pp. 704–710
39 De Marcellis, A., Ferri, G., Palange, E.: 'A novel analog autocalibrating phase-voltage converter for signal phase shifting detection', *IEEE Sens. J.*, 2011, **11**, pp. 259–266
40 Yonce, D.J., Bey, P.P.J., Fare, T.L.: 'A DC autonulling bridge for real-time resistance measurement', *IEEE Trans. Circuits Syst. I, Fundam. Theory Appl.*, 2000, **42**, pp. 273–278
41 Tadic, N., Gobovic, D.: 'Self-balancing linear bridge circuits with resistive mirrors for resistance measurement', *IEEE Trans. Instrum. Meas.*, 2000, **49**, pp. 1318–1325
42 Pradhan, R., Chatterjee, J., Mandal, M., Mitra, A., Das, S.: 'Monopolar impedance sensing microdevices for characterization of cells and tissue culture', *Sens. Lett.*, 2013, **11**, pp. 466–475
43 De Graaf, G., Wolffenbuttel, R.F.: 'Circuit for readout and linearization of sensor bridges'. Proc. 30th European Solid-State Circuits Conf., Leuven, Belgium, September 2004, pp. 451–454
44 Senani, R.: 'A new technique for inductance-to-time-period conversion using integrated circuit operational amplifiers', *IEEE Trans. Ind. Electron. Control Instrum.*, 1980, **IECI-27**, pp. 36–37
45 Senani, R.: 'Linear resistance-to-frequency conversion employing integrated circuit operational amplifiers', *Int. J. Electron.*, 1981, **50**, pp. 485–491
46 Senani, R.: 'On linear inductance-time and related conversions using IC op amps', *IEEE Trans. Ind. Electron.*, 1987, **IE-34**, pp. 292–293
47 Goras, L., Marcuta, C.: 'On linear inductance- and capacitance-time conversions using NIC-type configurations', *IEEE Trans. Ind. Electron.*, 1993, **40**, pp. 529–531
48 Goras, L., Marcuta, C.: 'Comment on 'A new technique for inductance-to-time-period conversion using integrated circuit operational amplifiers'', *IEEE Trans. Ind. Electron.*, 1985, **IE-32**, p. 85

49 Shin, D.-Y., Lee, H., Kim, S.: 'Improving the accuracy of capacitance-to-frequency converter by accumulating residual charges', *IEEE Trans. Instrum. Meas.*, 2011, **60**, pp. 3950–3955
50 Julsereewong, P., Julsereewong, A., Rerkratn, A., Pootharaporn, N.: 'Simple resistance-to-time converter with lead-wire-resistance compensation'. Proc. SICE Annual Conf., Waseda University, Tokyo, Japan, September 2011, pp. 2760–2763
51 Kabara, P., Thakur, S., Saileshwar, G., Baghini, M.-S., Sharma, D.-K.: 'CMOS low-noise signal conditioning with a novel differential resistance to frequency converter for resistive sensor applications'. Proc. IEEE Int. SoC Design Conf. (ISOCC), Jeju, South Korea, November 2011, pp. 298–301
52 Islam, T., Kumar, L., Uddin, Z., Ganguly, A.: 'Relaxation oscillator-based active bridge circuit for linearly converting resistance to frequency of resistive sensor', *IEEE Sens. J.*, 2013, **13**, pp. 1507–1513
53 Wang, Y., Chodavarapu, V.-P.: 'Design of CMOS capacitance to frequency converter for high-temperature MEMS sensors'. Proc. IEEE Sensors, Baltimore, USA, November 2013, pp. 1–4
54 Islam, T., Khan, A.-U., Akhtar, J.: 'Accuracy analysis of oscillator-based active bridge circuit for linearly converting resistance to frequency'. Proc. IEEE Int. Conf. on Multimedia, Signal Processing and Communication Technologies (IMPACT), Aligarh – Uttar Pradesh, India, November 2013, pp. 305–309
55 Nojdelov, R., Nihtianov, S.: 'Capacitive sensor interface with improved dynamic range and stability'. Proc. IEEE Int. Instrumentation and Measurement Technology Conf. (I2MTC), Montevideo, Uruguay, May 2014, pp. 1373–1376
56 D'Amico, A., Di Natale, C.: 'A contribution on some basic definitions of sensors properties', *IEEE Sens. J.*, 2001, **1**, pp. 183–190